OCEANIC RELICT TEXTURES IN THE MOUNT AVIC SERPENTINITES, WESTERN ALPS

Emanuele Fontana✉**, Matteo Panseri** and **Paola Tartarotti**

Dipartimento di Scienze della Terra "A. Desio", Università degli Studi di Milano, Italy.
✉ *Corresponding author, e-mail: emanuele.fontana@unimi.it*

Keywords: *Serpentinite, Ti-clinohumite, Piemonte ophiolite, Zermatt-Saas ophiolite. Western Alps.*

ABSTRACT

The Mount Avic serpentinites derive from mantle peridotites that have been involved in several geodynamic episodes, from their formation in the Jurassic Tethys, to the subduction event and suture in the Alpine chain. The main steps of their tectono-metamorphic evolution are inferred by investigating the texture and mineralogy of selected samples. Some serpentinite samples show relict textures and mineralogy related to the emplacement in the oceanic realm and to the early Alpine evolution. Olivine and clinopyroxene porphyroblasts preserve relict mantle textures. Magnetite crystals include relict chromite at their core. Abundant pseudomorphs of antigorite on former porphyroblasts are present. Mineral composition of the pseudomorphic serpentine partly inherits the composition of former minerals (e.g., relatively Ti-rich antigorite replacing pyroxene). These observations support the hypothesis that the Mount Avic serpentinites derive from original mantle porphyroclastic peridotites. An early formation of Ti-clinohumite during oceanic serpentinization of mantle peridotites at relatively high temperature conditions, followed by HP subduction-related Alpine recrystallization, is proposed. The late orogenic history is characterised by transposition accompanied by greenschist facies minerals crystallization. In these samples, antigorite represents the main mineral phase, marking a pervasive, often mylonitic, foliation. The last generation of serpentine, that occurs as yellow fibres filling late extension veins, was formed during a Neo-Alpine brittle-ductile deformation stage.

INTRODUCTION

Serpentinite is an important component of many ophiolite complexes; it represents the mantle portion of former oceanic lithosphere. The meta-ophiolites of the Western Alps (i.e., the Piemonte Ophiolitic Nappe) include several serpentinite sheets and large serpentinite masses, these latter commonly forming the base of ophiolitic sub-units (Bearth, 1967; Dal Piaz and Ernst, 1978; Pfeifer et al., 1989; Li et al., 2004). The Zermatt-Saas ophiolitic unit (Zermatt area and northern Aosta Valley) has been affected by at least four stages of metamorphic overprint, from hydration at the ocean floor through subduction-related high pressure (HP), and locally ultra-high pressure (UHP) conditions, to subsequent greenschist facies conditions after exhumation, and late hydrothermal alteration (Ernst and Dal Piaz, 1978; Reinecke, 1998; Desmons et al., 1999; Bucher et al., 2005; Martin et al., 2008). Early hydration of mantle peridotites is attested by the presence of relict pseudomorphs replacing the original mineral phases and textures (Rahn and Bucher, 1998; Li et al., 2004).

In the modern oceanic environments, most of the abyssal peridotites cropping out on the seafloor are more or less serpentinised. These mantle rocks commonly occur along axial valley, walls and transform fault scarps of slow to ultra-slow spreading systems (Mével, 2003 and refs. therein). The primary texture of abyssal peridotites is very often still recognisable, despite the extensive serpentinization, because most of these rocks are undeformed, i.e., they are altered under static conditions. The primary mineralogy of abyssal peridotites consists of olivine ± orthopyroxene ± clinopyroxene ± spinel. Olivine is replaced by serpentine in mesh textures, while orthopyroxene and, to a minor extent, clinopyroxene are replaced by bastite ± talc and/or amphibole (e.g., Aumento and Loubat, 1971; Prichard, 1979).

The rocks under investigation belong to the Piemonte Ophiolitic Nappe exposed in the southern Aosta Valley (Fig. 1). In this area, meta-ophiolites are comparable with the eclogitic Zermatt-Saas Unit, as defined in the Zermatt area and in the northern Aosta Valley (e.g., Martin and Tartarotti, 1989; Dal Piaz et al., 2001; Martin et al., 2008). The study area is dominated by a huge (nearly 180 km^2) dome consisting of mantle serpentinites (the Mount Avic massif; Fig. 1). Although serpentinites are a dominant component of the Piemonte Ophiolitic nappe, the literature has devoted more attention to the crustal portions of the ophiolitic complex, i.e., pelagic metasediments, metavolcanites and metagabbros. This is due to a more reliable record in such rocks of the P-T metamorphic conditions, providing diagnostic and quantitative thermobarometry evaluations. Former works focused on the serpentinites of the Western Alps meta-ophiolites mostly refer to the Zermatt-Saas area (e.g., Rahn and Bucher, 1998; Li et al., 2004), the Voltri Massif (e.g., Messiga et al., 1995, Scambelluri and Rampone, 1999; Hermann et al., 2000; Scambelluri et al., 2001; 2004), and the external border of the Lanzo Massif (e.g., Bodinier et al., 1986; Bodinier, 1988). Only few works describe the Mount Avic serpentinites (e.g., Diella et al., 1994; Tartarotti et al., 1998).

This paper provides a new detailed description of the texture and mineralogy of the Mount Avic serpentinites, consisting of serpentine (antigorite) and variable amounts of diopside, olivine, chlorite, tremolite, Ti-clinohumite, and magnetite. Similarly to the Zermatt-Saas area, the serpentinites of the southern Aosta Valley preserve records of their entire evolution, from the emplacement in the ocean to the present-day setting.

GEOLOGICAL FRAMEWORK

The Mount Avic massif (southern Aosta Valley, Italian Western Alps; Fig. 1) belongs to the Piemonte Ophiolitic

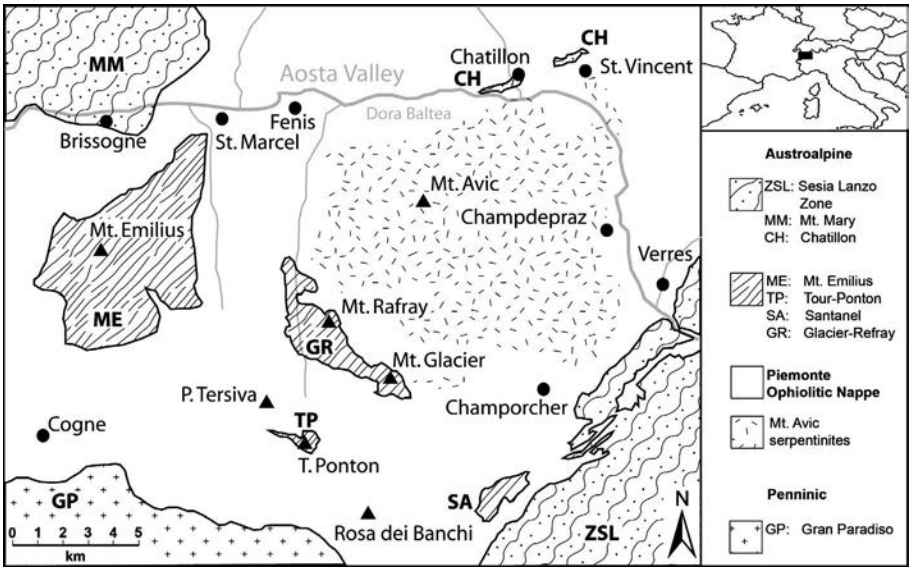

Fig. 1 - Simplified structural map of the mid Aosta Valley with location of the Mount Avic serpentinites (modified after Tartarotti et al., 1998).

Nappe which represents a fossil part of the Mesozoic Western Tethys oceanic lithosphere, i.e., the Piemontese-Ligurian basin (Elter, 1971; Dal Piaz and Ernst, 1978; Battiston et al., 1984; Ballévre et al., 1986; Dal Piaz, 1988; Vannay and Allemann, 1990; Ballévre and Merle, 1993; Martin et al., 1994; Reddy et al., 1999; Dal Piaz et al., 2001). The Western Tethys Ocean opened in Early Jurassic (Stampfli et al., 1991). The Eoalpine high-pressure event represents the evidence of the subduction stage taking place from ~130 Ma to ~40 Ma ago (Platt, 1986; Hunziker and Martinotti, 1987; Polino et al., 1990; Bowtell et al., 1994; Reinecke, 1998; Dal Piaz et al., 2001; Federico et al., 2007). The southward subduction of the Western Tethys beneath the Africa plate proceeded until the onset of the collision between the Africa and Eurasia Plates (Eocene-Oligocene). This stage (Mesoalpine event) was characterised by a barrovian metamorphism (Hunziker and Martinotti, 1987; Dal Piaz and Gosso, 1993; Reinecke, 1998, Amato et al., 1999; Federico et al., 2007). Since Late Oligocene (Neoalpine event), deformation in the Western Alps became mainly brittle and was accomodated along major fault lineaments and minor faults (Bistacchi et al., 2000; 2001; Bistacchi and Massironi, 2000).

The Piemonte Ophiolitic Nappe separates the Austroalpine units from the underlying Penninic nappes. Two main units compose the ophiolitic system: the Combin and the Zermatt-Saas Units, as defined in the Zermatt area (Switzerland) and in the northern Aosta Valley (Italy). These units are characterised by different lithologies as well as by a distinct metamorphic evolution (Dal Piaz and Ernst, 1978; Bearth and Schwander, 1981; Battiston et al., 1984; Ballèvre et al., 1986; Sartori, 1987; Dal Piaz, 1988; Dal Piaz et al., 2001; Martin and Cortiana, 2001). A large part of the Zermatt-Saas ophiolites is represented by serpentinites. Huge mantle-derived antigorite serpentinite bodies occur in the northern side of the Aosta Valley (Mt. Rosso di Verra-Breithorn Massif; e.g., Dal Piaz, 1969; Dal Piaz and Ernst, 1978; Dal Piaz et al., 1980). Other serpentinitic bodies crop out in the southern Aosta Valley (Mount Avic massif), in the Orsiera-Rocciavrè ophiolite (Pognante, 1979), in the Monviso complex (Lombardo and Pognante, 1982), and in the Voltri Massif (Piccardo et al., 1988; Scambelluri and Rampone, 1999; Hermann et al., 2000; Scambelluri et al., 2001). The Lanzo Massif is a well preserved peridotite body cropping out in the southwestern Piemonte zone (Piccardo et al., 2005; 2007).

In the southern Aosta Valley, to the South of the Aosta-Ranzola fault, the Piemonte Ophiolitic Nappe is mainly composed of serpentinized peridotites exposed in the Mount Avic massif, which include chloriteschists and rodingitic dykes, minor eclogitic mafic rocks, and metasediments (Martin et al., 1994; Tartarotti et al., 1998; Fontana, 2005; see also Panseri et al., 2008, this volume). Serpentinites consist of antigorite schists bearing Ti-clinohumite, diopside, talc, tremolite.

METHODS

The present paper is based on a geological field survey performed in the Mount Avic massif area which has also provided a structural-lithological map (see also Panseri et al., 2008, this volume). Although this work is focused on serpentinites, other lithologies (eclogitic mafic rocks, calcschists and rodingitic dykes) were also sampled and investigated from the outcrop-scale to micro-scale using both polarised optical microscope and scanning electronic microscope (SEM).

Energy dispersive spectroscopic (EDS) analyses were carried out at the Consiglio Nazionale delle Ricerche (CNR) - Dipartimento di Scienze della Terra (Milano University) and were performed on a Cambridge System Stereoscan 360 SEM. Operating conditions were: 20kV accelerating voltage; 25mm working distance; 0.4nA specimen current; 10s counting time. The correction program used is SAF4 (Pouchou and Pichoir, 1985).

FIELD OBSERVATIONS

The Mount Avic massif represents one of the largest ultramafic units of the Western Alps. The study area (Fig. 2) is located in the southwestern part of the Mount Avic serpentinite body, where serpentinite is the most common lithology. The ophiolitic crustal section is poorly represented and consists of partly retrogressed eclogitic mafic rocks, rodingites, chloriteschist and talcschist lenses, and of calcschist (Fontana, 2005; Panseri et al., 2008, this volume).

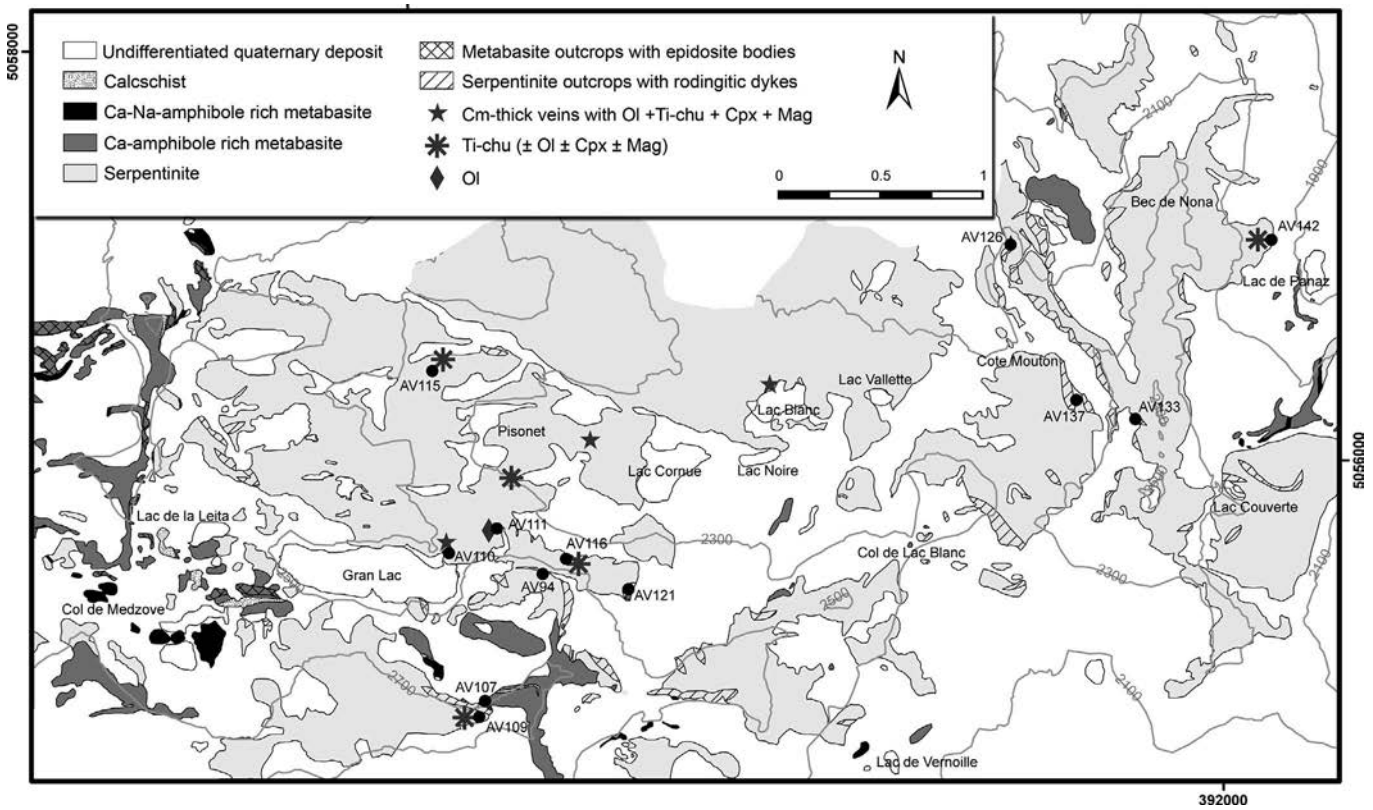

Fig. 2 - Lithological map of the study area derived from original geological field survey (Fontana, 2005), and location of the studied samples (see also Table 1). UTM coordinate, datum ED 1950, zone 32N.

At the outcrop scale, serpentinites often show a pervasive alteration coat with a light-brown, ochre or reddish color. The color of fresh-fracture surfaces depends on the rock texture which varies from mylonitic to slightly foliated or massive, up to fibrous (from black or dark to light shade of green, respectively). Slightly foliated or massive serpentinite is the most common type. Mylonitic serpentinites crop-out near the contact with other rocks.

Two main foliations (S_1 and S_2) related to two different stages of the Alpine evolution (D_1 and D_2, respectively) were recognised in the field. S_1 in serpentinites occurs only locally (e.g. Gran Lac, Lac de Leser; Fig 2) and it is deformed by a D_2 phase, producing S_2 crenulation cleavage. S_2 (not always preserved) is the main fabric which is parallel to the contacts between serpentinites and the other ophiolitic rocks.

Serpentinite is mainly composed of serpentine, commonly associated with sub-millimetric magnetite grains. A peculiar feature of the Mount Avic serpentinite is the abundance, inside S_1, of cm-thick ribbons and boudins composed of olivine, Ti-clinohumite, diopside, and magnetite. These veins are particularly well preserved between Gran Lac and Lac Blanc (Fig. 2). Millimetric-thick veins filled with yellow serpentine fibres cut the two foliations and are then likely related to the very late brittle deformation.

Several bodies of metamorphosed mafic rocks (ranging from few metres to few hundreds of metres in size) occur within serpentinites. The mafic rocks are composed either of Ca-amphibole, albite, chlorite and epidote ± fuchsite, and rare pyrite (type A), or of Ca-Na-amphibole, Na-amphibole, albite, epidote, rare biotite and white mica (type B). Type A-rocks are coarser-grained and their texture varies from flaser to nematoblastic or locally lepidoblastic (metagabbro?); prasinite is occasionally observed. Type B-rocks are fine-grained and may include eclogitic relics (almandine, omphacite and rutile); they are interpreted as metabasalts.

The contact between the two types of mafic rocks is gradual. In contrast, the contacts between the mafic bodies and serpentinites are sharp and clearly tectonic, being aligned along the regional schistosity (S_2).

Several metric bodies of chloriteschist and rodingite (garnet, vesuvianite, diopside, chlorite and epidote) and few decimetric talcschist lenses occur (Panseri et al., 2008, this volume). Moreover, a m-scale slice of calcschist composed of white mica, plagioclase, calcite, garnet and epidote, was also mapped (south and west of Gran Lac; Fig. 2).

TEXTURES AND PETROGRAPHY OF THE MOUNT AVIC SERPENTINITES

The textures of the Mount Avic serpentinites likely represent the final result of a complex reworking developed during multiple phases of tectonic and metamorphic overprinting. The Mount Avic serpentinites show heterogeneous textural features. In the field there is a gradual change in grain size from very fine-grained (mylonitic texture) to coarse-grained (slightly foliated or massive texture). Consequently, a clear distinction among different serpentinite types is often difficult to be achieved. Thin-section investigations were addressed to recognizing different fabrics, their relative chronology, and the associated minerals (Table 1).

At the micro scale, two main distinct foliations are common: the first one (S_1) is mostly recognizable in relict chevron fold hinges inside S_2 crenulation cleavage which represents the main schistosity (Fig. 3a). Within serpen-

Table 1 - Table of mineral occurrences from selected samples of serpentinite.

Sample[a]	UTM X[b]	UTM Y[c]	Minerals (with relative modal abundance)[d]
AV94	388661	5055445	Srp (98%) + Spl (<2%) [Am]
AV107	388337	5054810	Srp (79%) + Am (10%) + Spl (5%) + Chl (3%) + Cb (<3%) [Pn, Cpx]
AV109	388374	5054757	Srp (70%) + Cpx (15%) + Chl (8%) + Spl (5%) + Ti-chu (2%) [Ol]
AV110	388202	5055547	Srp (75%) + Ol (10%) + Cpx (6%) + Ti-chu (5%) + Spl (4%)
AV111	388436	5055668	Ol (50%) + Srp (41%) + Spl (8%) [Chl]
AV115	388123	5056442	Srp (70%) + Ti-chu (15%) + Chl (10%) + Spl (3%) + Ol (2%)
AV116	388776	5055519	Chl (60%) + Srp (23%) + Ti-chu (10%) + Spl (6%) [Cb]
AV121	389083	5055371	Srp (70%) + Cb (15%) + Am (10%) + Spl (5%)
AV126	390955	5057055	Srp (90%) + Spl (10%)
AV133	391567	5056202	Srp (77%) + Chl (10%) + Spl (8%) + Cpx (5%)
AV137	391265	5056309	Srp (75%) + Spl (15%) + Cb (10%) [Chl]
AV142	392235	5057079	Cpx (45%) + Chl (20%) + Ti-chu (15%) + Srp (15%) + Spl (5%)

a) Sample name. b) and c) Sample GPS coordinates (UTM coordinate, datum ED 1950, zone 32N). d) Mineral occurrences; round brackets: relative modal abundance; square brackets: rare minerals (<1%). Am: amphibole; Cb: carbonate; Chl: chlorite; Cpx: clinopyroxene; Ol: olivine; Spl: spinel; Srp: serpentine; Ti-chu: Ti-clinohumite. Mineral abbreviations according to Siivola and Schmid (2007).

tinites, S_1 is marked by serpentine, clinopyroxene, olivine, Ti-clinohumite, and magnetite. S_2-foliation within serpentinites is marked by serpentine ± amphibole ± chlorite + opaque minerals. This foliation is often a spaced cleavage (Passchier and Trouw, 1998), in which serpentine forms both cleavage domains and lens-shaped microlithons (Fig. 3b) that may contain microfolds of the earliest foliation or fabric elements with no preferred orientation. Transposed or rootless folds related to D_1 phase are common, and are generally marked by spinel alignment.

Serpentine is the most abundant mineral, with the exception of some samples (samples AV111, AV116, and AV142; Table 1). Within S_2, serpentine occurs both as isooriented acicular crystals (within cleavage domains) and as sub-millimetric prismatic or anhedral grains (usually within microlithons). Yellowish microfibres of serpentine (probably chrysotile) fill the late extension veins which crosscut all previous textures (Fig. 3c). Aggregates of large grains of serpentine frequently form sub-rounded or rhombic pseudomorphic sites (Figs. 3d, 3e).

Opaque minerals (mainly magnetite, modal abundance ≤ 15%; Table 1) are ubiquitous; they usually form millimetric pods, disseminated along the foliation. In samples AV 94 and AV 126, mm-sized magnetite crystals form fold hinges related to S_1. Some grains include thin laths of serpentine. Centimetric aggregates of magnetite together with chlorite are pseudomorphic on a pre-existing mineral (Fig. 3f). Opaque minerals partially replace Ti-clinohumite together with serpentine.

Chlorite occurs in the samples AV 107, AV 109, AV 111, AV 115, AV 116, AV 133, AV137, and AV142 (modal amounts between 10 and 40%; Table 1) yielding mm-thick sheets parallel to the foliation. Chlorite also grows around opaque mineral aggregates.

Clinopyroxene occurs in the samples AV 107, AV 109, AV 110, and AV133 (relative modal abundance ≤ 15%; Table 1). Sample AV142 shows the highest clinopyroxene abundance (~ 45%; Table 1). Clinopyroxene crystals exhibit two different textures. Cpx I (millimetric) is prismatic and highly fractured. It includes opaque crystals filling fractures or growing along the internal cleavage (Fig. 4a). Cpx I porphyroblasts also show mechanical twins. Oval-shaped aggregates of Cpx I are common. Cpx II (≤ 0.5mm) is acicular (occasionally round-shaped; samples AV109 and AV110) and aligned along the foliation. Cpx II grows after Cpx I (dynamic crystallization). These neoblasts occur in contact with Cpx I porphyroblasts or make elongated crystal aggregates (Fig. 4b).

Olivine occurs within samples AV 109, AV 110, AV 115 (modal abundance ≤ 10%; Table 1) and AV 111 (modal abundance ~ 50%; Table 1).

Olivine is present as round-shaped and intensely fractured centimetric porphyroblasts (Ol I) as well as smaller rounded grains (Ol II; Fig. 4c). Olivine I crystals show intracrystalline deformation attested by the presence of subgrains (deformation lamellae?; Fig. 4c). Ol II neoblasts derive from dynamic recrystallization of Ol I. Neoblasts either rim Ol I porphyroblasts or occur in the finer–grained portions of the rock in association with serpentine crystals.

Ti-clinohumite occurs in samples AV 109, AV 110, AV 115, AV 116, and AV142 (always with modal abundance ≤ 15%; Table 1). Ti-clinohumite is found either as isolated scattered millimetric crystals bordered by spinel, or as cm-thick boudinaged ribbons together with olivine and pyroxene. These ribbons and boudins are wrapped, and in some cases penetrated, by S_2-foliation (Fig. 4d, e). Ti-clinohumite exhibits two different textures: Ti-chu I consists of mm- to cm-sized porphyroblasts (pseudomorphic?) in assemblage with Cpx I, serpentine and spinel (Fig. 4f). Ti-chu II crystallised after Ti-chu I (dynamic crystallization) and occurs as finer-grained sub-rounded or prismatic crystals (Figs. 4d, 4e).

Samples AV 94, AV 107, and AV 121 contain amphibole (modal abundance ≤ 10%; Table 1) which shows two distinct textures: coarse-grained pseudomorphic amphibole (Am I) replaces Cpx I and preserves the pyroxene texture and shape; finer-grained amphibole (Am II) forms acicular or sub-rounded crystals.

Carbonate occurs within samples AV 107 and AV 116 (modal abundance < 3%), AV 121 (~ 15%), and AV 137 (~ 10%; Table 1). It is characterised by prismatic centimetric crystals or microcrystalline aggregates growing along the S_2 foliation or filling fractures.

Summing up, thin-section observations suggest that some serpentine samples exhibit relict textures that are preserved from the tectonic reworking of late Alpine tectono-metamorphic phases. These textures include: pseudomorphic tex-

tures (serpentine or amphibole replacing previous porphyroblasts), subgrains in olivine porphyroblasts as possible mantle-related texture, porphyroblasts as possible heritage of the protolith mineral association. By contrast, more elaborated textures do not show structural or minerlogical relics, being the product of tectonic reworking during D_2 and later phases.

COMPOSITION OF MINERALS

Serpentine

The composition of natural serpentine has generally small deviance from the ideal formula: $Mg_3[Si_2O_5](OH)_4$ (Wicks and O'Hanley, 1988). Substitution is mainly performed by Al both in tetrahedral and octahedral site (tscher-

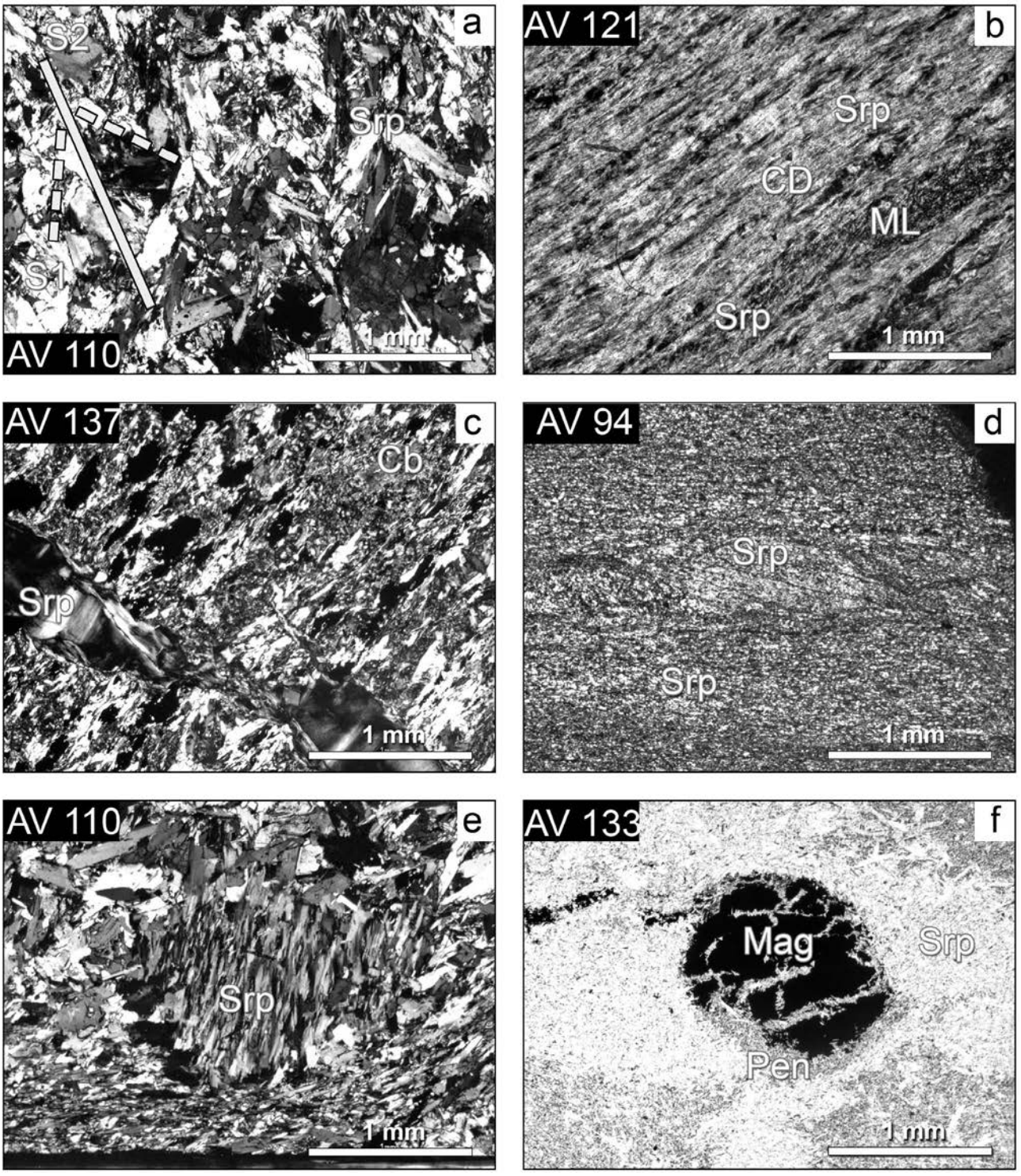

Fig. 3 - Photomicrographs of representative serpentinite samples. a) Chevron microfolds in crenulated S_1 foliation marked by serpentine crystals (Srp). S_2 crenulation cleavage is also shown. Crossed nicols. b) Spaced cleavage defined by fine-grained serpentine (Srp) crystals. S_2 cleavage domain (CD) dominates the fabric. S_1 is transposed and not recognizable within the microlithons (ML). Crossed nicols. c) Late extension veins filled with fibrous serpentine (Srp; chrysotile?) crosscutting previous textures. Cb: carbonate. Crossed nicols. d) and e) Pseudomorphic serpentine (Srp) replacing an older crystal (mantle pyroxene?). In Fig. 3d, the oval-shaped antigorite pseudomorph preserves an internal cleavage. Crossed nicols. f) Pseudomorphic magnetite (Mag) and chlorite (penninite, Pen) aggregate replacing an older crystal. Plane light. Mineral abbreviations according to Siivola and Schmid (2007).

mak substitution). These substitutions imply a solid solution and/or interstratification among serpentine, chlorite and amesite (septechlorite; Nelson and Roy, 1958; Chernosky et al., 1988; Bailey, 1988a; 1988b; Bailey et al., 1995).

Distinction between different serpentine varieties (e.g., lizardite, crysotile and antigorite) is not possible without using X-ray diffraction techniques (Wicks and O'Hanley, 1988). However, antigorite is the high pressure-high temperature serpentine variety (e.g. Evans, 1976; Barnicoat and Fry, 1986; Ulmer and Trommsdorf, 1995; Wunder and Schreyer, 1997; Hilairet et al., 2006) and, on the basis of mineral paragenesis of the studied serpentinites, we infer

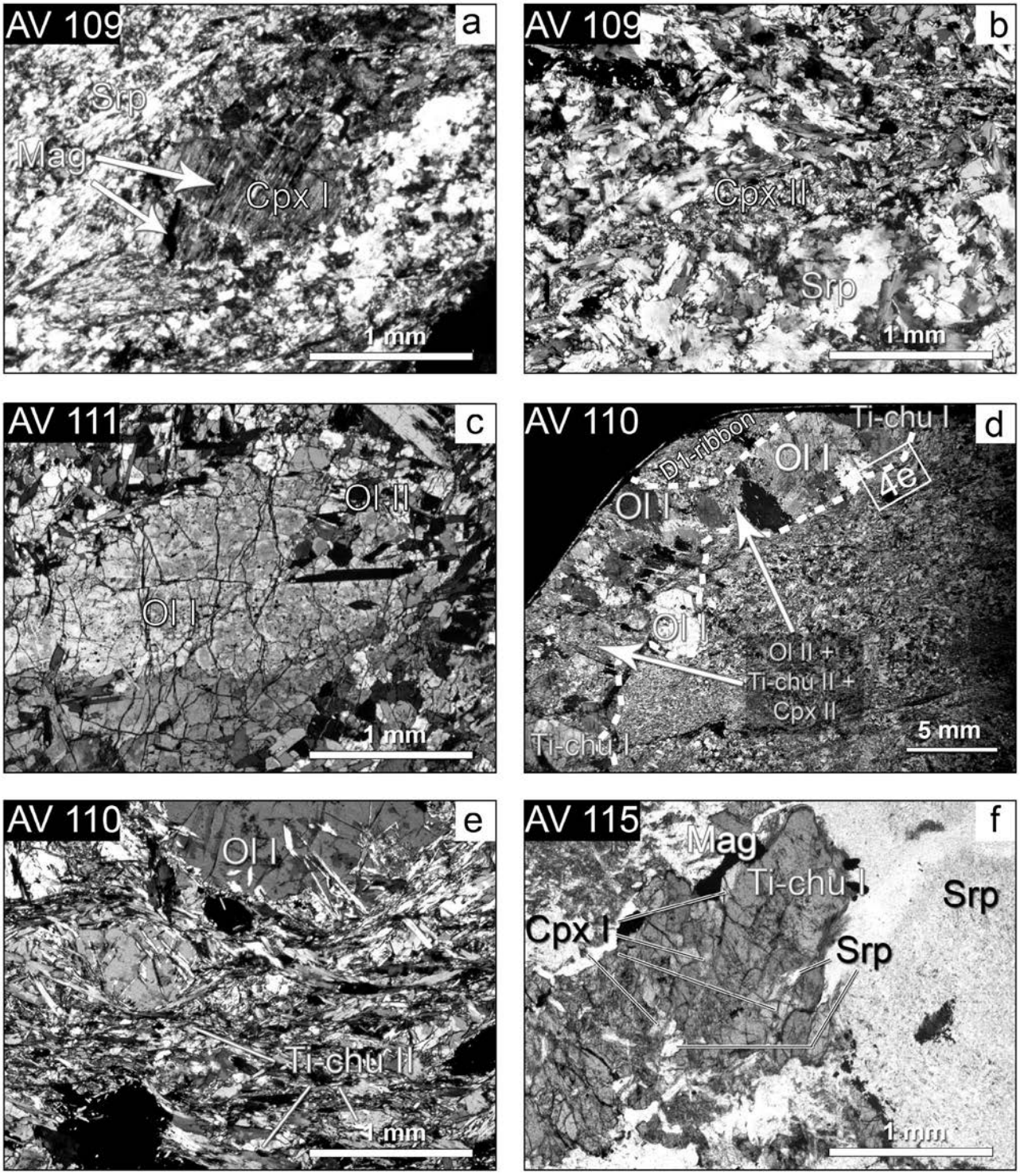

Fig. 4 - Photomicrographs of representative serpentinite samples. a) Relict clinopyroxene (diopside) porphyroblast (Cpx I) with internal cleavage inherited from primary pyroxene, partly filled with magnetite (Mag). Crossed nicols. b) Elongated aggregate of sub-millimetric neoblasts of clinopyroxene (diopside, Cpx II). Crossed nicols. c) Olivine porphyroblast (Ol I) with internal subgrains. Ol I is rimmed by neoblasts of Ol II. Crossed nicols. d) Boudinaged ribbon (related to D_1 deformation phase) composed of olivine (Ol I + Ol II), Ti-clinohumite (Ti-chu I + Ti-chu II), and clinopyroxene neoblasts (Cpx II). Inset shows the location of Figure 4e. Crossed nicols. e) Detail of Fig. 4d, showing porphyroblastic olivine (Ol I) and Ti-clinohumite neoblasts (Ti-chu II) wrapped by S_2 foliation. Crossed nicols. f) Porphyroblast of Ti-clinohumite (Ti-chu I) associated with relict diopside (Cpx I), serpentine (Srp) and magnetite (Mag). Crossed nicols. Mineral abbreviations according to Siivola and Schmid (2007).

that most part of serpentine is antigorite, as also observed by Li et al. (2004) in the Zermatt-Saas area. There is a relationship between major elements content within the analysed serpentine and its texture (Table 2). In fact, pseudomorphic antigorite, as well as serpentine that fills late veins, contains relatively higher Ti. Antigorite included in spinel crystal cores has a variable Ti content (Fig. 5), and shows higher amounts of Cr_2O_3 (ranging between 0.30 and 0.73 wt%) with respect to serpentine from the other textural sites (Table 2). Serpentine filling late veins has a low tschermak component ($Al^{IV}Al^{VI}$ - $Mg_{-1}Si_{-1}$) whereas in other textural sites it has a variable tschermak component (Fig. 6 and Table 2).

Spinel

Magnetite is the most common spinel occurring in the analysed serpentinites. The largest (mm-sized) magnetite crystals were selected for SEM-EDS analyses (Table 3). These crystals are characterised by a Cr-rich core and a Cr-poor rim (Fig. 7 and Table 3). A slight Al-Mg depletion from core to rim in these crystals were detected (Fig. 8 and Table 3).

Chlorite

Within the serpentinite, the chlorite has a penninitic composition (Table 4). Penninite is a solid solution of amesite and septechlorite. Talc-chlorite was also analysed (analysis 137-23; Table 4). Penninite and talc-chlorite are close to serpentine composition, being characterised by low Al- and high Mg- and Si-contents with respect to clinochlore (Hey, 1954; Wiewiora and Weiss, 1990). Penninite crystals are characterised by high Cr contents (Cr_2O_3 ranging between ~ 1.5 and 10.4 wt%; Table 4).

Pyroxene

The chemical composition of the analysed pyroxene crystals is very homogeneous (Table 5). No orthopyroxene was found. Clinopyroxene has a composition very close to

Table 2 - Representative serpentine analyses from selected samples of serpentinite.

	serpentine				
Sample	AV110	AV111	AV137	AV137	AV137
Analysis	110-129	111-29	137-25	137-9	137-15
Occurrence	s1	s2	ps	v	in
	core	core	core	core	core
Na2O	0.00	0.00	0.00	1.28	0.00
MgO	37.60	38.79	40.21	40.52	39.76
Al2O3	2.94	1.93	0.67	0.32	1.64
SiO2	42.51	42.37	44.63	42.47	44.22
SO3	0.01	0.00	0.00	0.00	0.00
K2O	0.04	0.00	0.00	0.00	0.00
CaO	0.06	0.04	0.02	0.00	0.00
TiO2	0.00	0.00	0.17	0.17	0.06
Cr2O3	0.06	0.14	0.27	0.00	0.73
MnO	0.18	0.06	0.00	0.00	0.04
FeO	3.48	2.02	1.10	1.73	2.64
NiO	0.11	0.00	0.00	0.00	0.00
Total Ox	**86.99**	**85.36**	**87.07**	**86.49**	**89.11**
Si	1.99	2.00	2.06	2.00	2.01
Al	0.16	0.11	0.04	0.02	0.09
Fe2	0.14	0.08	0.04	0.07	0.10
Mg	2.62	2.74	2.76	2.84	2.70
Ca	0.00	0.00	0.00	0.00	0.00
Na	0.00	0.00	0.00	0.12	0.00
K	0.00	0.00	0.00	0.00	0.00
Ti	0.00	0.00	0.01	0.01	0.00
Mn	0.01	0.00	0.00	0.00	0.00
Cr	0.00	0.01	0.01	0.00	0.03
Ni	0.03	0.00	0.00	0.00	0.00
Total Cat	**4.93**	**4.94**	**4.91**	**5.05**	**4.93**
Al IV	0.01	0.00	0.00	0.00	0.00
Si+Al IV	2.00	2.00	2.06	2.00	2.01
Al IV/Si	0.01	0.00	0.00	0.00	0.00
Al VI	0.15	0.11	0.04	0.01	0.09
2Al VI/Mg	0.12	0.08	0.03	0.01	0.07
Oct Site	2.95	2.93	2.858	3.05	2.92

Formula calculated on the basis of 7 equivalent oxygens. Sample: thin section label. Analysis: analysis number. Occurrence: s2- serpentine along S_2; s1- serpentine along S_1; ps- pseudomorphic serpentine; v- serpentine filling vein; in- serpentine included in magnetite with Cr-rich core. Location of the analysis spot is indicated.

Table 3 - Representative magnetite analyses from selected samples of serpentinite.

	magnetite				
Sample	AV111	AV126	AV126	AV137	AV137
Analysis	111-44	126-50	126-51	137-12	137-13
	core	intermediate	rim	rim	core
TiO2	0.21	0.38	0.07	0.07	0.47
Al2O3	0.43	0.20	0.00	0.06	0.06
Cr2O3	29.53	13.61	0.99	4.32	24.80
Fe2O3	38.25	54.18	66.56	64.73	44.24
FeO	25.29	28.39	29.84	27.59	21.25
MnO	0.86	1.24	0.38	0.44	2.44
MgO	3.73	1.07	0.31	2.12	5.16
NiO	0.00	0.31	0.26	0.00	0.00
SiO2	0.40	0.09	0.20	0.20	0.16
Total Ox	**98.71**	**99.46**	**98.62**	**99.55**	**98.59**
Ti	0.01	0.01	0.00	0.00	0.01
Al	0.02	0.01	0.00	0.00	0.00
Cr	0.87	0.41	0.03	0.13	0.73
Fe3	1.07	1.55	1.95	1.85	1.23
Fe2	0.79	0.90	0.97	0.88	0.66
Mn	0.03	0.04	0.01	0.01	0.08
Mg	0.21	0.06	0.02	0.12	0.29
Ni	0.00	0.01	0.01	0.00	0.00
Si	0.02	0.00	0.01	0.01	0.01
Total Cat	**3.00**	**3.00**	**3.00**	**3.00**	**3.00**
R2 site	1.00	1.00	1.00	1.00	1.00
R3 site	2.00	2.00	2.00	2.00	2.00
Fe2/Fe2+Mg	79.18	93.72	98.15	87.94	69.81
Cr/Cr+Al	97.87	97.84	100.00	97.97	99.61
Fe3/Fe3+Cr+Al	54.68	78.76	98.46	93.32	62.85
Ti/Ti+Al+Cr	0.67	2.57	6.64	1.53	1.78
Fe/R2	76.81	88.91	96.14	86.64	63.62
Mn/R2	2.68	4.03	1.24	1.42	7.71
Mg/R2	20.51	6.11	1.82	11.94	28.67
Ni/R2	0.00	0.96	0.80	0.00	0.00
R2TiO4	0.61	1.11	0.22	0.21	1.33
RAl2O4	0.96	0.46	0.00	0.14	0.14
RCr2O4	44.09	20.55	1.54	6.53	36.52
RFe2O4	54.35	77.89	98.25	93.13	62.01

Formula calculated on the basis of 4 oxygens. Sample: thin section label. Analysis: analysis number. Location of the analysis spot is indicated.

Table 4 - Representative chlorite analyses from selected samples of serpentinite.

	chlorite				
Sample	AV107	AV111	AV111	AV137	AV137
Analysis	107-127	111-39	111-43	137-23	137-26
Name	penninite	penninite	penninite	talc-chlorite	penninite
	core	core	core	core	core
Na2O	0.00	0.00	0.00	0.00	0.00
MgO	31.64	33.69	28.04	38.00	34.80
Al2O3	12.47	11.25	8.24	3.11	7.70
SiO2	33.34	33.14	25.69	41.30	35.10
K2O	0.04	0.00	0.00	0.00	0.08
CaO	0.01	0.00	0.04	0.08	0.00
TiO2	0.02	0.04	0.00	0.09	0.04
Cr2O3	1.85	2.15	10.45	1.01	1.55
MnO	0.02	0.02	0.40	0.05	0.00
FeO	5.92	3.43	9.50	2.92	4.07
NiO	0.00	0.00	0.00	0.00	0.00
Ox Total	**85.32**	**83.72**	**82.37**	**86.58**	**83.35**
Si	6.52	6.54	5.60	7.78	6.97
Al	2.88	2.62	2.12	0.69	1.80
Fe2	0.97	0.57	1.73	0.46	0.68
Mg	9.23	9.91	9.11	10.67	10.30
Ca	0.00	0.00	0.01	0.02	0.00
Na	0.00	0.00	0.00	0.00	0.00
K	0.01	0.00	0.00	0.00	0.02
Ti	0.00	0.01	0.00	0.01	0.01
Mn	0.00	0.00	0.07	0.01	0.00
Cr	0.29	0.34	1.80	0.15	0.24
Ni	0.00	0.00	0.00	0.00	0.00
Cat Total	**19.90**	**19.98**	**20.44**	**19.79**	**20.01**
Al IV	1.48	1.46	2.40	0.22	1.03
Al VI	1.40	1.16	0.00	0.47	0.77
Tet	8.00	8.00	8.00	8.00	8.00
Oct	11.89	11.98	12.73	11.79	11.99
Al IV/Si	0.23	0.22	0.43	0.03	0.15
2AlVI /Mg+Fe2	0.27	0.22	0.00	0.08	0.14
Fe/Fe+Mg	0.10	0.05	0.16	0.04	0.06

Formula calculated on the basis of 28 equivalent oxygens. Sample: thin section label. Analysis: analysis number. Name: chlorite nomenclature (Hey, 1954). Location of the analysis spot is indicated.

Table 5 - Representative clinopyroxene analyses from selected samples of serpentinite.

	clinopyroxene				
Sample	AV109	AV109	AV109	AV110	AV142
Analysis	109-01	109-02	109-03	110-124	142-08
Generation	I	I	II	II	I
	core	rim	core	core	core
SiO2	49.23	49.20	49.51	55.91	49.11
TiO2	0.58	0.72	0.77	0.06	0.72
Al2O3	6.20	4.01	5.09	0.00	7.53
Cr2O3	0.79	1.08	1.03	0.05	1.05
Fe2O3	4.87	4.28	5.21	0.00	2.34
FeO	0.00	0.00	0.00	0.71	1.15
MnO	0.00	0.00	0.00	0.08	0.00
MgO	16.48	18.04	16.31	17.97	14.71
CaO	21.13	21.17	21.75	26.11	21.61
Na2O	0.91	0.70	0.96	0.04	0.93
Ox Total	**100.19**	**99.20**	**100.63**	**100.93**	**99.15**
Si	1.79	1.81	1.80	2.00	1.80
Ti	0.02	0.02	0.02	0.00	0.02
Al	0.27	0.17	0.22	0.00	0.33
Cr	0.02	0.03	0.03	0.00	0.03
Fe3	0.13	0.12	0.14	0.00	0.07
Fe2	0.00	0.00	0.00	0.02	0.04
Mn	0.00	0.00	0.00	0.00	0.00
Mg	0.89	0.99	0.89	0.96	0.81
Ca	0.82	0.84	0.85	1.00	0.85
Na	0.06	0.05	0.07	0.00	0.07
Cat Total	**4.01**	**4.03**	**4.02**	**4.00**	**4.00**
Al IV	0.21	0.17	0.20	0.00	0.20
Al VI	0.06	0.00	0.02	0.00	0.13
Tet	2.00	1.99	2.00	2.00	2.00
Oct	1.13	1.16	1.10	0.99	1.08
M2	1.01	1.05	1.02	1.01	1.00
Mg/Mg+Fe2	100.00	100.00	100.00	97.83	95.79
Quad	76.98	82.60	78.59	99.69	75.64
Wo	47.96	45.75	48.94	50.53	50.28
En	52.04	54.25	51.06	48.40	47.63
Fs	0.00	0.00	0.00	1.07	2.09

Formula calculated on the basis of 6 oxygens. Sample: thin section label. Analysis: analysis number. Generation: I, II refers to porphyroblast and neoblast, respectively. Location of the analysis spot is indicated.

the diopside end member. No variations in chemical compositions were found in clinopyroxene porphyroblasts (Cpx I) and in neoblasts (Cpx II).

Olivine

Olivine composition varies from Fo_{90} to Fo_{96}, and this variation does not depend on the olivine generation (Table 6). In a few cases, olivine neoblasts (Ol II) is Ti-enriched (TiO_2 within Ol I is absent or less than 0.1 wt%, while in Ol II TiO_2 ranges between 0.1 and 0.3 wt%).

Ti-clinohumite

There are not relevant chemical differences between Ti-chu I and Ti-chu II (Table 7) A slight decrease in Ti content was detected within Ti-chu II ($TiO_2 \geq 4$ wt% in Ti-chu I; $TiO_2 \leq 4$ wt% in Ti-chu II). This result agrees with data obtained in another sector of the Mount Avic massif (Tartarotti and Bocchio, unpublished data).

Amphibole

All amphibole crystals analysed in serpentinite samples are tremolite (according to Leake et al., 1997's nomenclature), including pseudomorphs after Cpx I porphyroblasts (Am I) and acicular amphibole crystals (Am II).

Carbonate

Microcrystalline carbonate filling fractures is composed of calcite, whereas carbonate crystals along the S_2 foliation have a dolomite composition.

DISCUSSION

On the basis of thin-section observations and mineral chemistry results obtained from the studied samples, two major types of textures can be distinguished: 1) relict textures, i.e., porphyroblasts, pseudomorphs replacing former porphyroblastic minerals, subgrains in olivine porphyroblasts; 2) reworked textures, lacking relict structures and mineralogy, as a product of tectonic reworking during the late Alpine phases. The two groups of textures allow to discuss the nature of the serpentinite protolith, its oceanic evolution in the Western Tethys, and the subsequent evolution during the Alpine subduction and exhumation.

Table 6 - Representative olivine analyses from selected samples of serpentinite.

	olivine				
Sample	AV110	AV110	AV111	AV110	AV111
Analyses	110-123	110-026D	111-32	110-035D	111-40
Generation	I	I	I	II	II
	core	core	core	core	core
SiO2	41.44	40.86	41.62	41.37	42.17
TiO2	0.00	0.00	0.00	0.05	0.00
Al2O3	0.10	0.00	0.00	0.15	0.17
Cr2O3	0.05	0.00	0.00	0.00	0.00
FeO	8.80	9.36	4.89	8.59	4.09
MnO	0.51	0.52	0.19	0.35	0.16
MgO	49.43	49.12	53.25	49.74	52.91
CaO	0.00	0.01	0.00	0.00	0.06
K2O	0.04	0.04	0.00	0.00	0.00
NiO	0.25	0.32	0.00	0.08	0.00
Total Ox	**100.61**	**100.24**	**99.95**	**100.32**	**99.57**
Si	1.01	1.00	1.00	1.00	1.01
Ti	0.00	0.00	0.00	0.00	0.00
Al	0.00	0.00	0.00	0.00	0.01
Cr	0.00	0.00	0.00	0.00	0.00
Fe2	0.18	0.19	0.10	0.17	0.08
Mn	0.01	0.01	0.00	0.01	0.00
Mg	1.79	1.79	1.90	1.80	1.89
Ca	0.00	0.00	0.00	0.00	0.00
K	0.00	0.00	0.00	0.00	0.00
Ni	0.01	0.01	0.00	0.00	0.00
Total Cat	**2.99**	**3.00**	**3.00**	**2.99**	**2.99**
Mg/Mg+Fe	0.91	0.90	0.95	0.91	0.96
Fe/Mg+Fe	0.09	0.10	0.05	0.09	0.04
Mg/R2+	0.90	0.89	0.95	0.91	0.96
Fe/R2+	0.09	0.10	0.05	0.09	0.04
Mn/R2+	0.01	0.01	0.00	0.00	0.00
Forsterite	90.44	89.85	94.91	90.84	95.68
Fayalite	9.03	9.60	4.89	8.80	4.15
Tephroite	0.53	0.54	0.20	0.36	0.17

Formula calculated on the basis of 4 oxygens. Sample: thin section label. Analysis: analysis number. Generation: I, II refers to porphyroblast and neoblast, respectively. Location of the analysis spot is indicated.

Table 7 - Representative Ti-clinohumite analyses from selected samples of serpentinite.

	Ti-clinohumite				
Sample	AV110	AV110	AV110	AV110	AV110
Analysis	110-119	110-029D	110-030D	110-036D	110-037D
Generation	I	I	I	II	II
	core	rim	core	core	rim
SiO2	36.90	36.82	36.29	36.89	37.44
TiO2	4.57	4.62	4.39	3.98	3.65
Al2O3	0.00	0.00	0.00	0.14	0.00
FeO	8.86	8.65	8.60	9.17	8.76
MnO	0.62	0.45	0.47	0.64	0.46
NiO	0.28	0.14	0.35	0.17	0.13
MgO	46.56	47.54	47.48	48.16	48.66
CaO	0.00	0.00	0.00	0.00	0.00
K2O	0.00	0.08	0.00	0.00	0.05
H2O	1.67	1.69	1.74	1.88	1.95
Total Ox	**99.44**	**99.99**	**99.33**	**101.03**	**101.08**
Si	4.07	4.02	3.99	3.99	4.04
Ti	0.38	0.38	0.36	0.32	0.30
Al	0.00	0.00	0.00	0.02	0.00
Fe2	0.82	0.79	0.79	0.83	0.79
Mn	0.06	0.04	0.04	0.06	0.04
Ni	0.02	0.01	0.03	0.02	0.01
Mg	7.65	7.74	7.78	7.77	7.82
Ca	0.00	0.00	0.00	0.00	0.00
K	0.00	0.01	0.00	0.00	0.01
H	1.23	1.23	1.28	1.35	1.40
Total Cat	**13.00**	**13.00**	**13.00**	**13.00**	**13.00**

Formula calculated on the basis of 9 equivalent oxygens. Sample: thin section label. Analysis: analysis number. Generation: I, II refers to porphyroblast and neoblast, respectively. Location of the analysis spot is indicated.

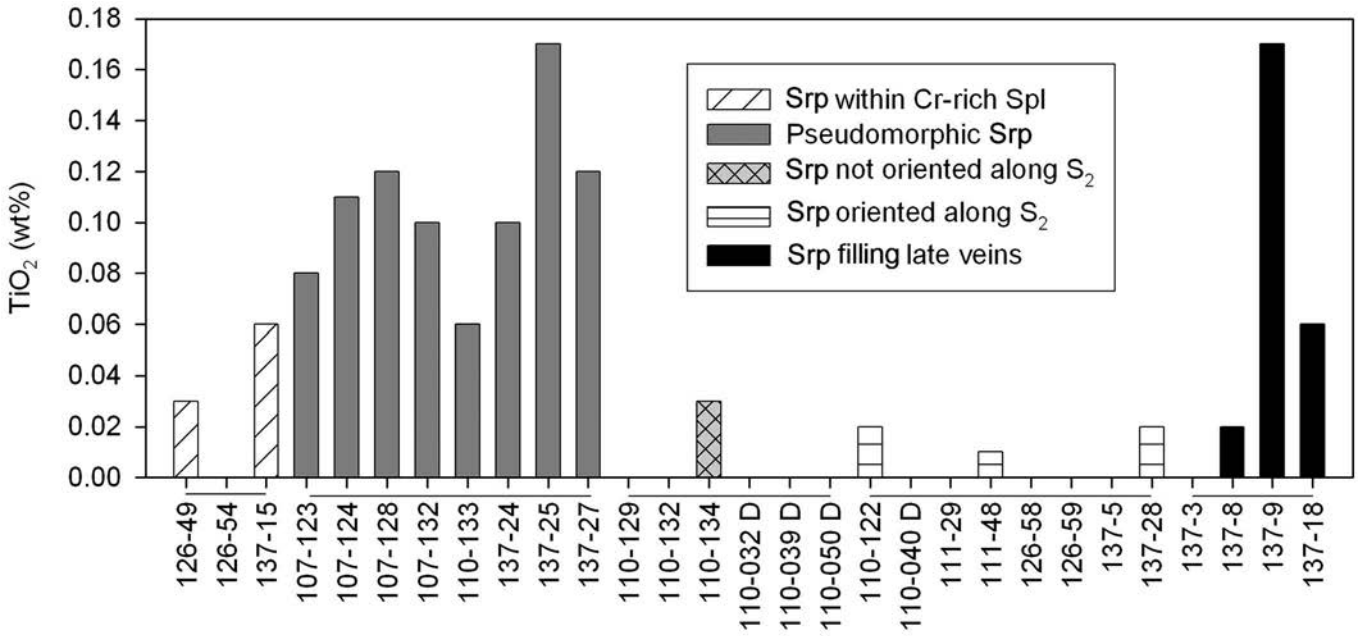

Fig. 5 - TiO_2 content in the analysed serpentine. Note that pseudomorphic serpentine (Srp) as well as serpentine filling late veins have higher TiO_2 content. Spl: spinel. Mineral abbreviations according to Siivola and Schmid (2007).

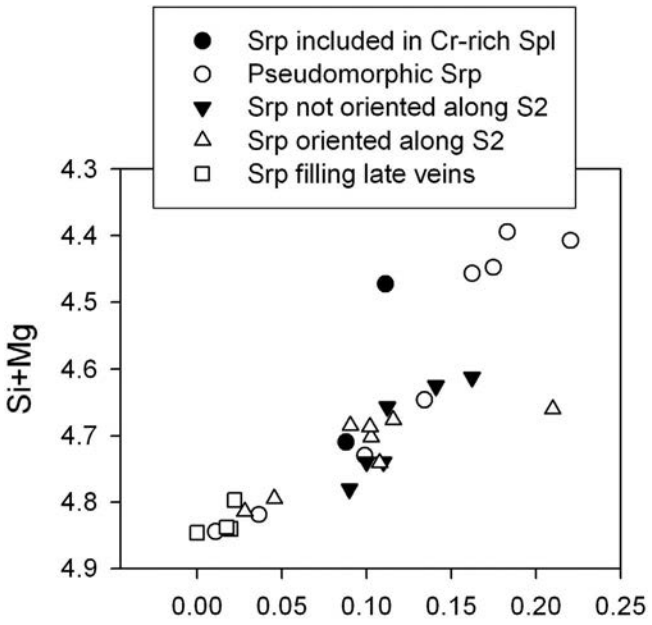

Fig. 6 - Tschermak substitution within serpentine (atoms p.f.u.). Note that serpentine (Spr) filling late veins has a low tschermak component. Spl: spinel. Nomenclature and abbreviations according to Spear (1994) and Sivola and Schmid (2007).

Origin of the Mount Avic serpentinite

The nature of the protolith of the studied samples is here inferred mostly by considering the relict textures and their mineral chemistry.

Ol I and Cpx I porphyroblasts are here interpreted as mantle textural relics, as suggested by their size, highly fractured surfaces, and intra-crystalline deformation. In fact, subgrains inside Ol I recall intracrystalline "deformation lamellae" (Den Tex, 1969; Mercier and Nicolas, 1975). Their formation depends on dislocation alignment forming along parallel glide lines within the crystal. Such a texture is very common in porphyroclastic mantle tectonites (Mercier and Nicolas, 1975; Nicolas and Poirier, 1976). We infer that recrystallization of mantle olivine into Ol I did not completely delete the original mantle structure. Mantle olivine from present-day oceans have almost homogeneous compositions (Fo ranging between 90% and 91%; e.g., Bonatti and Michael, 1989; Dick, 1989; Tartarotti et al., 2002). The composition of Ol I and Ol II in the Mount Avic serpentinite is only in part comparable with that of oceanic mantle olivine. In fact, Fo ranges between 90% and 95% (see previous section). Variability of Fo content in olivine from our samples could reflect slight variable compositions of the primary chemical system possibly coupled with oxidation of fayalite component to magnetite during metamorphic recrystallization (see Li et al., 2004).

Cpx I porphyroblasts inherits the texture of mantle clinopyroxene. Although the original chemistry is not preserved (as described above, all the analysed pyroxenes have a chemical composition very close to the diopside end-member), characteristic internal structures of mantle clinopyroxene like mechanical twinning and exolution lamellae (Gueguen and Nicolas, 1980; Tartarotti et al., 2002) are preserved within Cpx I and replaced by opaque minerals.

Besides olivine and clinopyroxene, other minerals interpreted as mantle relics occur. Magnetite with a Cr-rich core may derive from an original chromite. Chromite commonly forms during the first stages of magmatic crystallization due to magmatic segregation within mafic and ultramafic rocks. Diella et al. (1994) have suggested that magnetite ore bodies occurring in the Mount Avic serpentinites derive from chromitites that were generated during the mantle emplacement beneath the ocean crust, and subsequently transformed during the Alpine metamorphic evolution. Accordingly, the Cr-rich core analysed in our magnetite crystals can be interpreted as relict chromite in ultramafic rocks.

Oceanic serpentinization

The mantle peridotite of the Mesozoic Tethyan Ocean might have been exposed at the ocean floor, as already suggested by Driesner (1993) and Tartarotti et al. (1998), similarly to mantle peridotites of the present-day slow- and ultra-slow spreading ridges and transform faults (e.g., Karson, 1991; Mével et al., 1991; Cannat et al., 1997; Lagabrielle et al., 1998), allowing a pervasive serpentinization. Serpentinization proceeds through the progressive substitution of olivine and pyroxene by serpentine (lizardite; Prichard, 1979). Generally, olivine is the first mineral to be replaced during serpentinization (Wicks and Whittaker, 1977; Prichard, 1979; Macdonald and Fyfe, 1985), giving rise to the so-called "hour-glass" or "mesh" texture (Aumento and Loubat, 1971; Prichard, 1979). Consequently, serpentine of the studied serpentinites may derive either by recrystallization of oceanic serpentine or by hydration of minerals during the subduction and exhumation of mantle slices in the Alpine orogen. By contrast, fresh olivine porphyroblasts (Ol I) preserved in our samples might have escaped oceanic serpentinization and then recrystallised during the Alpine history, as observed by Li et al. (2004) in the Zermatt-Saas Unit. In the studied serpentinites, antigorite forms oval-shaped

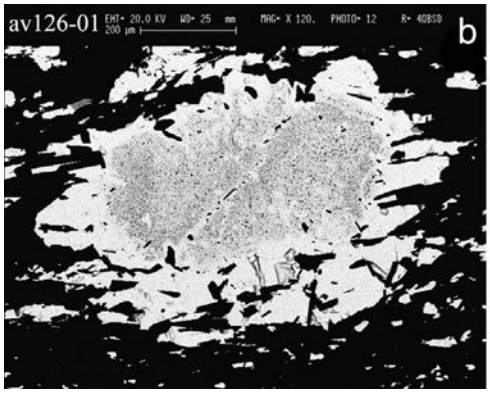

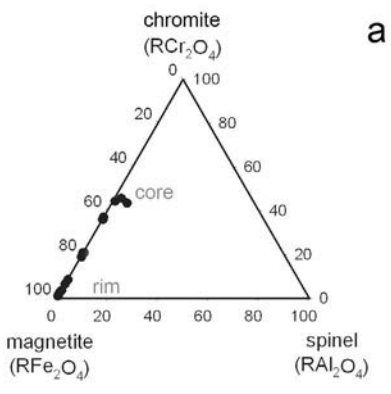

Fig. 7 - Spinel with Cr-rich core. a) Backscattered image of magnetite. Grey field within spinel is due to high Cr contents. b) Spinel classification diagram made on the base of trivalent ions (Al, Fe, and Cr; excluding ulvospinel), with plot of the EDS analys. Cr is concentrated toward the core of the spinel.

pseudomorphs derived from pyroxene. These sites are often deformed and elongated, but pyroxene internal cleavage is almost always preserved (see Fig. 3b). These pseudomorphs have often relative high Ti-contents, supporting the hypothesis of a mantle pyroxene origin for these sites. Antigorite + diopside (with characteristic internal cleavage; Cpx I) + magnetite (often observed within clinopyroxene miming exolution lamellae) + Ti-clinohumite ± chlorite (see Fig. 4f) replace clinopyroxene of likely mantle origin. This association has also been observed by Rahn and Bucher (1998) within serpentinites sampled along the Hörnli ridge (Matterhorn, Zermatt-Saas Unit). These Authors suggest the following schematic reaction for the mantle clinopyroxene breakdown during oceanic serpentinization:

$Cpx + H_2O + O_2 \rightarrow$ Ti-chu + Atg + Di + Mag (1)

Thisreaction is responsible for the formation of Ti-clinohumite during serpentinization of the oceanic lithosphere.

Trommsdorf and Evans (1980) have estimated an upper stability limit of Ti-clinohumite in association with antigorite and diopside at temperatures ≤ 520 °C and pressures of 3 kbars, and a lower limit at approximately 380 °C. The maximum pressure at which serpentinization occurs depends on the geodynamic setting. According to the maximum depth attained by the Moho at spreading ridges, serpentinites may form at a maximum depth of 10 km, i.e., at a maximum pressure of 3 kb (see review in Mével, 2003). As oceanic serpentinization may take place at temperatures as high as 500°C (Alt, 1995; Agrinier and Cannat, 1997; Alt and Shanks, 1998), such conditions are compatible with the Ti-clinohumite stability field as inferred by Trommsdorff and Evans (1980). Despite antigorite crystallization is uncommon during oceanic serpentinization, such serpentine variety has been reported in places in the present-day ocean crust (e.g. Miyashiro et al., 1969; Agrinier and Cannat, 1997, Ribeiro Da Costa et al., 2008; see also Mével, 2003). Although the reaction (1) may theoretically occur during oceanic metamorphism, it is also possible that the serpentine produced during this reaction was lizardite, subsequently replaced by antigorite during the prograde subduction path,

Scambelluri and Rampone (1999) infer a different genesis for Ti-clinohumite. They suggest high pressure conditions for the crystallization of this mineral within Fe-Ti-gabbros included in serpentinised ultramafites of the Western Liguria. According to these Authors, ocean floor Mg-metasomatism would have produced intense chloritization of magmatic plagioclase within Fe-Ti-gabbros. During the high-pressure orogenic evolution, breakdown of chlorite, ilmenite and augite might have lead to crystallization of Ti-clinohumite. Although some mafic rocks of the Mount Avic are comparable with Fe-Ti-gabbros (Fontana, 2005), in the study area there are not apparent relations between mafic rocks and Ti-clinohumite-rich zones (spatial relations are instead observed between some mafic rocks and rodingites; see Panseri et al., 2008, this volume). Moreover, Ti-clinohumite from our samples is never associated with mafic minerals. Instead, Ti-clinohumite is often found next to Cr-rich spinel which is likely included in peridotites.

The occurrence of Ti-clinohumite in ultamafic rocks closely associated with mafic rocks has been reported within the high pressure meta-peridotites of Erro-Tobbio (Voltri Massif, Western Liguria), in assemblage with antigorite, diopside, magnetite, chlorite and olivine (Messiga et al., 1995; Scambelluri et al., 1997 and 2004). Both Ti-clinohumite and olivine of Erro-Tobbio are always fine-grained and related to high pressure conditions (Scambelluri et al., 1997). In contrast with the Erro-Tobbio rocks, in the Mount Avic serpentinites, olivine and Ti-clinohumite occur together within ribbons as porphyroblasts and do not show evidence of textural equilibrium (see Fig. 4d and e). In literature, the occurrence of Ti-clinohumite crystallised under HP conditions within ultramafic rocks are described in association with olivine (e.g., Trommsdorff and Evans, 1980; Scambelluri et al., 1997 and 2004; Groppo and Compagnoni, 2007). The samples studied here show the occurrence of Ti-clinohumite in absence of olivine (see Fig. 4f). As the reaction (1) proposed by Rahn and Bucher (1998) involves oxidation, it is more likely referable to the oceanic environment, as already discussed by Rahn and Bucher (1998). We therefore suggest a possible oceanic origin for Ti-clinohumite of the Mount Avic serpentinites, although a subduction origin for such mineral cannot be ruled out.

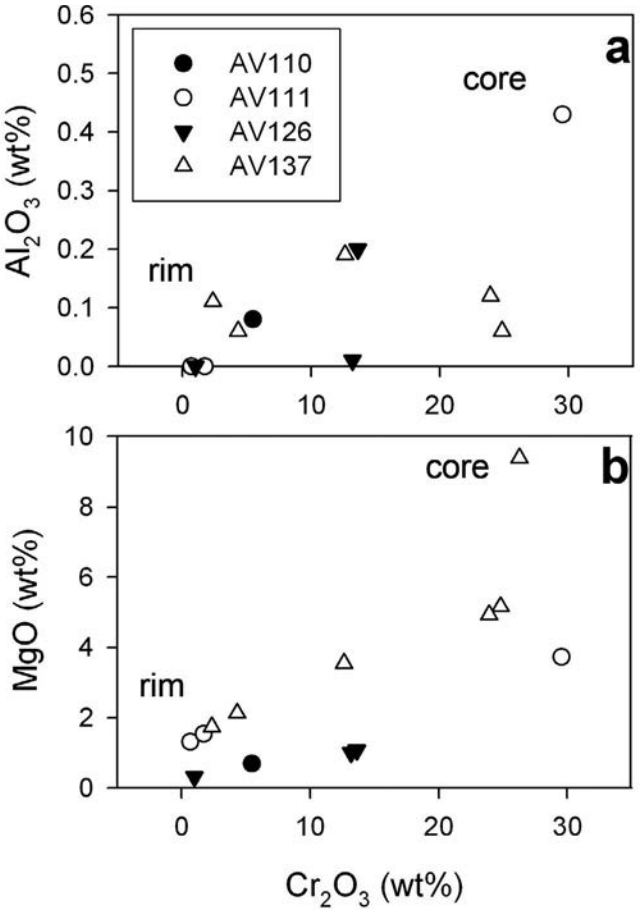

Fig. 8 - Relationship between Cr_2O_3, Al_2O_3, and MgO contents within magnetite. From core to rim, Cr_2O_3, Al_2O_3 and MgO decrease.

In spite of the small amount of Ti in mantle clinopyroxene (Robinson, 1980; Rahn and Bucher, 1998), Ti released during the clinopyroxene breakdown have been totally included into Ti-clinohumite during reaction (1). We also suggest that Al and Mg have been transferred to serpentine and chlorite, whilst Fe have been incorporated into magnetite. Recrystallised clinopyroxene (Cpx I) probably retained all Ca of the primary mantle clinopyroxene.

Alpine evolution

Thin-sections observations suggest that the studied rocks have been affected by at least two phases during the Alpine

history, D_1 and D_2, producing foliations S_1 and S_2, respectively. During D_1, Cpx I as well as Ol I (still preserving mantle internal structures) have recrystallised into sub-millimetric Cpx II and Ol II crystals, respectively. Ti-chu II has grown from Ti-chu I. Centimetric ribbons and boudins composed of olivine, Ti-clinohumite and clinopyroxene likely developed during D_1. Spinel has been replaced by magnetite, probably during the prograde subduction phase as attested by the occurrence of Cr-rich core (Diella et al., 1994). D_1 is here interpreted as an early deformation phase related to the eo-Alpine subduction.

Throughout Late Eocene and Oligocene, greenschist facies metamorphism, related to collision and exhumation phases, overprinted the Eo-Alpine HP metamorphic minerals in the Piemonte Ophiolitic Nappe (see e.g., Reinecke, 1998; Federico et al., 2007). In our samples, D_2 phase has developed a more or less pervasive foliation marked by greenschist facies minerals (e.g., tremolite, antigorite). During this stage, coarsening of antigorite through recrystallization occurred, as suggested by Li et al. (2004) for the Zermatt serpentinites. The last generation of serpentine (occurring as yellow fibres filling late extension veins) crystallised during brittle-ductile deformation related to the Neo-Alpine stage (e.g., Bistacchi et al., 2000; Bistacchi and Massironi, 2000).

Conclusions

The Mount Avic serpentinites derive from mantle peridotites that have been involved in several geodynamic episodes, from their formation in the Jurassic Thethys and oceanic alteration, to subduction and suture in the Alpine chain. The main steps of this complex tectono-metamorphic evolution are inferred by investigating the texture and mineralogy of selected samples.

Some serpentinite samples show relict textures and mineralogy referable to the early oceanic evolution. Textural features of Ol I and Cpx I are interpreted as relict mantle textures. This interpetation is also supported by mineral composition of olivine, that is partly comparable with that of olivine from present-day oceanic lithosphere, and by the occurrence of relict chromite inside magnetite crystals. Abundant pseudomorphs of antigorite on former porphyroblasts support the hypothesis that the Mount Avic serpentinites derive from original mantle peridotites. Mineral composition of pseudomorphic serpentine and/or chlorite partly inherits the composition of former minerals (e.g., relatively higher Ti content in antigorite replacing pyroxene). We speculate that during ocean seafloor and/or subseafloor serpentinization the original mantle peridotites have not been completely altered before their subduction at the beginning of the Africa and Europe Plates convergence. Serpentinization probably occurred not only at the seafloor but possibly at deeper levels, leading to the crystallization of Ti-clinohumite. Although extensively recrystallised during the Alpine evolution, Ti-clinohumite of the Mount Avic serpentinites is here interpreted to be of oceanic origin. During the early Alpine evolution, mantle textures recrystallised with formation of olivine, diopside, and Ti-clinohumite neoblasts.

The late orogenic history is characterised by transpositive foliation associated with greenschist facies minerals. In these samples, antigorite represents the main mineral phase, marking a pervasive, often mylonitic, foliation. The last generation of serpentine, that occurs as yellow fibres filling late extension veins, was formed during brittle-ductile deformation related to the Neo-Alpine stage.

ACKNOWLEDGEMENTS

We are grateful to S. Martin and P. Agard; their helpful comments and careful reviews allowed us to considerably improve this paper.

REFERENCES

Agrinier P. and Cannat M., 1997. Oxygen-isotope constraints on serpentinization processes in ultramafic rocks from the mid-atlantic ridge (23°N). In: J.A. Karson, M. Cannat, D.J. Miller and D. Elthon (Eds.), Proceed. O. D. P. Sci. Results, 153: 381-388.

Alt J.C., 1995. Subseafloor processes in mid-ocean ridge hydrothermal systems. In: S.E. Humphris, R. Zierenberg, L. Mullineaux and R. Thomson (Eds.), Seafloor hydrothermal systems: Physical, chemical, biological and geological interactions within hydrothermal systems. Geophys. Monogr., Am. Geophys. Union, 91: 85-114.

Alt J.C. and Shanks W.C., 1998. Sulfur in serpentinised oceanic peridotite: serpentinization processes and microbial sulfate reduction. J. Geophys. Res., 103: 9917-9929.

Amato J.M., Johnson C.M., Baumgartner L.P. and Beard B.L., 1999. Rapid exhumation of the Zermatt-Saas ophiolite deduced from high-precision SmNd and RbSr geochronology. Earth Planet. Sci. Lett., 171 (3): 425-438.

Aumento F. and Loubat H., 1971. The Mid-Atlantic Ridge near 45°N: serpentinised ultramafic intrusions. Can. J. Earth Sci., 8: 631-663.

Bailey S.W., 1988a. Chlorites: Structures and crystal chemistry. Mineral. Soc. Am. Rev. Mineral., 19: 347-403.

Bailey S.W., 1988b. Structures and compositions of other trioctahedral 1:1 phyllosilicates. Mineral. Soc. Am. Rev. Mineral., 19: 169-188.

Bailey S.W., Banfield J.F., Barker W.W. and Katchan G., 1995. Dozyite, a 1:1 regular interstratification of serpentine and chlorite. Am. Mineral., 80: 65-77.

Ballévre M., Kienast J.R., and Vuichard J.P., 1986. La "Nappe de la Dent Blanche" (Alpes Occidentales): deux unités austroalpin indipéndantes. Ecl. Geol. Helv., 79 (1): 57-74.

Ballévre M. and Merle O., 1993. The Combin fault: compressional reactivation of a Late Cretaceous-Early Tertiary detachment fault in the Western Alps. Schweiz. Mineral. Petrogr. Mitt., 73 (2): 205-227.

Barnicoat A.C. and Fry N., 1986. High-pressure metamorphism of the Zermatt-Saas ophiolite, Switzerland. J. Geol. Soc. London, 143: 607-618.

Battiston P., Benciolini L., Dal Piaz G.V., De Vecchi G., Marchi G., Martin S., Polino R. and Tartarotti, P., 1984. Geologia di una traversa dal Gran Paradiso alla zona Sesia-Lanzo in alta Val Soana, Piemonte. Mem. Soc. Geol. It., 29: 209-232.

Bearth P., 1967. Die Ophiolite der Zone von Zermatt-Saas Fee. Beitr. Geol. Karte Schweiz, 132: 1-130.

Bearth P. and Schwander H., 1981. The post-Triassic sediments of the ophiolite zone Zermatt-Saas Fee and the associated manganese mineralization. Ecl. Geol. Helv., 74 (1): 189-205.

Bistacchi A., Dal Piaz G.V., Massironi M., Zattin, M. and Balestrieri M.L., 2001. The Aosta-Ranzola extensional fault system and Oligocene: present evolution of the Austroalpine-Penninic wedge in the northwestern Alps. Intern. J. Earth Sci., 90 (3): 654-667.

Bistacchi A., Eva, E., Massironi M. and Solarino S., 2000. Miocene to Present kinematics of the NW-Alps: evidences from remote sensing, structural analysis, seismotectonics and thermochronology. J. Geodyn., 30 (1-2): 205-228.

Bistacchi A. and Massironi M., 2000. Post-nappe brittle tectonics and kinematic evolution of the north-western Alps: an integrated approach. Tectonophysics, 327 (3-4): 267-292.

Bodinier J.L., 1988. Geochemistry and petrogenesis of the Lanzo peridotite body, western Alps. Tectonophysics, 149: 67-88.

Bodinier J.L., Giraud M., Dupuy C. and Dostal J., 1986. Geochemistry of basic dikes in the Lanzo massif (Western Alps): petrogenetic and geodynamic implications. Tectonophysics, 128: 77-95.

Bonatti E. and Michael P.J., 1989. Mantle peridotites from continental rifts to ocean basins to subduction zones. Earth Planet. Sci. Lett., 91: 297-311.

Bowtell S.A., Cliff R.A. and Barnicoat A.C., 1994. Sm-Nd isotopic evidence on the age of eclogitization in the Zermatt-Saas ophiolite. J. Metam. Geol., 12 (2): 187-196.

Bucher K., Fazis Y., De Capitani C. and Grapes R., 2005. Blueschists, eclogites, and decompressional assemblages of the Zermatt-Saas ophiolites: high-pressure metamorphism of subducted Tethys lithosphere. Am. Mineral., 90: 821-835.

Cannat M., Lagabrielle Y., Bougault H., Casey J., de Coutures N., Dmitriev L. and Fouquet Y., 1997. Ultramafic and gabbroic exposures at the Mid-Atlantic Ridge: geological mapping in the 15°N region. Tectonophysics, 279: 193-213.

Chernosky J.V. Jr., Berman R.G. and Bryndzia L.T. 1988. Stability, phase relations, and thermodynamic properties of chlorite and serpentine group minerals. Mineral. Soc. Am. Rev. Mineral., 19: 295-346.

Dal Piaz G.V., 1969. Filoni rodingitici e zone di reazione a bassa temperatura al contatto tettonico tra serpentine e rocce incassanti nelle Alpi occidentali italiane. Rend. Soc. It. Min. Petr., 27: 437-477.

Dal Piaz G.V., 1988. Revised setting of the Piedmont zone in the northern Aosta valley, Western Alps. Ofioliti, 13 (2-3): 157-162.

Dal Piaz G.V., Cortiana G., Del Moro A., Martin S., Pennacchioni G. and Tartarotti P., 2001. Tertiary age and paleostructural inferences of the eclogitic imprint in the Austroalpine outliers and Zermatt-Saas Ophiolite, Western Alps. Int. J. Earth Sci., 90: 668-684.

Dal Piaz G.V., Di Battistini G., Gosso G. and Venturelli G., 1980. Rodingitic gabbro dykes and rodingitic reaction zones in the upper Valtournanche-Breuil area, Piemonte Ophiolite nappe, Italian Western Alps. Arch. Sci. Genève, 33 (2-3): 161-179.

Dal Piaz G.V. and Ernst W.G., 1978. Areal geology and petrology of eclogites and associated metabasites of the Piemonte ophiolite nappe, Breuil-St. Jacques area, Italian Western Alps. Tectonophysics, 51 (1-2): 99-126.

Dal Piaz G.V. and Gosso G., 1993. Some remarks on evolution of the Alpine lithosphere. Quaderni Geodin. Alpina Quatern., 2: 93-101.

Den Tex E., 1969. Origin of ultramafic rocks, their tectonic setting and history: a contribution to the discussion of the paper "The origin of ultramafic and ultrabasic rocks" by P.J. Wyllie. Tectonophysics, 7: 457-488.

Desmons J., Compagnoni R., Cortesogno L. with the collaboration of Frey M., Gaggero L, Dellagiovanna G., Seno S. and Radelli L., 1999. Alpine metamorphism of the western Alps. I. Middle to high P/T metamorphism. Schweiz. Mineral. Petrogr. Mitt., 79: 89-110.

Dick H.J.B., 1989. Abyssal peridotites, very slow spreading ridges and oceanic ridge magmatism. In: A.D. Sanders and M.J. Morris (Eds.), Magmatism in the ocean basins. Geol. Soc. London Spec. Publ., 42: 71-105.

Diella V., Ferrario A. and Rossetti P., 1994. The magnetite ore deposits of the southern Aosta valley: chromitite transformed during an Alpine metamorphic event. Ofioliti, 19 (2a): 247-256.

Driesner T., 1993. Aspects of petrographical, structural and sTable isotope geochemical evolution of ophicarbonate breccias from ocean floor to subduction and uplift: an example from Chatillon, Middle Aosta Valley, Italian Alps. Schweiz. Mineral. Petrogr. Mitt., 73 (1): 69-84.

Elter G., 1971. Schistes lustrés et ophiolites de la zone piémontaise entre Orco et Doire Baltée (Alpes Garies). Hypothèses sur l'origine des ophiolites. Géol. Alpine, 47 (2): 147-169.

Ernst W.G. and Dal Piaz G.V., 1978. Mineral parageneses of eclogitic rocks and related mafic schists of the Piemonte ophiolite nappe,Breuil-St. Jacques area, Italian Western Alps. Am. Mineral., 63 (7-8): 621-640.

Evans B.W., 1976. Stability of chrysotile and antigorite in the serpentinite multisystem, Schweiz. Mineral. Petrogr. Mitt., 56: 79-93.

Federico L., Crispini L., Scambelluri M. and Capponi G., 2007. Ophiolite mélange zone records exhumation in a fossil subduction channel. Geology, 35 (6): 99-502.

Fontana E., 2005. Evoluzione oceanica e alpina delle serpentiniti del massiccio del Monte Avic (Valle d'Aosta). Tesi di laurea, unpubl., Univ. Studi Milano, 295 pp.

Gueguen Y. and Nicolas A., 1980. Deformation of Mantle Rocks. Ann. Rev. Earth Planet. Sci., 8: 119-144. doi: 10.1146/annurev.ea.08.050180.001003.

Groppo C., and Compagnoni R., 2007. Metamorphic veins from the serpentinites of the Piemonte Zone, western Alps, Italy: a review. Per. Mineral., 76: 127-153.

Hermann J., Müntener O. and Scambelluri M., 2000. The importance of serpentinite mylonites for subduction and exhumation of oceanic crust. Tectonophysics, 327 (3-4): 225-238.

Hilairet N., Daniel I. and Reynard B., 2006. Equation of state of antigorite, stability field of serpentines, and seismicity in subduction zones. Geophys. Res. Lett., 33: L02302, doi:10.1029/2005GL024728.

Hunziker J.C. and Martinotti G., 1987.Geochronolgy and evolution of the Western Alps: a review. Mem. Soc. Geol. It., 29: 43-56.

Karson J.A., 1991. Seafloor spreading on the Mid-Atlantic Ridge: implications for the structure of ophiolites and oceanic lithosphere produced in slow-spreading environments. In: J. Malpas, E.M. Moores, A. Panayiotou and C. Xenophontos (Eds.), Proceed. Symp. Troodos 1987, Geol. Survey Dept. Nicosia, p. 547-555.

Lagabrielle Y., Bideau D., Cannat M. Karson J.A. and Mével C., 1998. Ultramafic-mafic plutonic rock suites exposed along the Mid-Atlantic Ridge (10°N-30°N). Symmetrical-asymmetrical distribution and implications for seafloor spreading processes. In: W.R. Buck, P.T. Delaney, J.A. Karson and Y. Lagabrielle (Eds.), Faulting and magmatism at mid-ocean ridges. AGU Geophys. Monog, 106: 153-176.

Leake B.E., Woolley A.R., Arps C.E.S., Birch W.D., Gilbert M.C., Grice, J.D., et al., 1997. Nomenclature of amphiboles: report of the Subcommittee on Amphiboles of the International Mineralogical Association, Commission on New Minerals and Mineral Names. Am. Mineral., 82: 1019-1037.

Li X.P., Rahn M. and Bucher K., 2004. Serpentinites of the Zermatt-Saas ophiolite complex and their texture evolution. J. Metam. Geol., 22: 159-177.

Lombardo B. and Pognante U., 1982. Tectonic implications in the evolution of the western Alps ophiolite metagabbros. Ofioliti, 2: 371-394.

Macdonald A.H. and Fyfe W.S., 1985. Rate of serpentinization in seafloor environments. Tectonophysics, 116 (1-2): 123-135.

Martin S. and Cortiana G., 2001. Influence of the whole-rock composition on the crystallization of sodic amphiboles (Piemonte zone, Western Alps). Ofioliti, 26 (2b): 445-456.

Martin S., Rebay G., Kienast J.R. and Mével C., 2008. An eclogitised oceanic palaeo-hydrothermal field from the St. Marcel valley (italian Western Alps). Ofioliti, 33 (1): 49-63.

Martin S. and Tartarotti P., 1989. Polyphase HP metamorphism in the ophiolitic glaucophanites of the lower St. Marcel Valley (Aosta, Italy). Ofioliti 14 (2): 135–156.

Martin S., Tartarotti P. and Dal Piaz G.V., 1994. The mesozoic ophiolites of the Alps: a review. Boll. Geofis. Teor. Appl., 36 (141-144): 175-219.

Mercier J.-C.C. and Nicolas, A., 1975. Textures and fabrics of upper mantle peridotites as illustrated by xenoliths from basalts. J. Petrol., 16: 454-487.

Messiga B., Scambelluri M. and Piccardo G.B., 1995. Chloritoid-bearing assemblages in mafic systems and eclogite-facies hydration of alpine Mg-Al metagabbros (Erro-Tobbio Unit, Ligurian Western Alps). Eur. J. Mineral., 7 (5): 1149-1167.

Mével C., 2003. Serpentinization of abyssal peridotites at mid-ocean ridges. C.R. Geosci., 335: 825-852.

Mével C., Cannat M., Gente P., Marion E., Auzende J.-M. and Karson J.A., 1991. Emplacement of deep rocks on the west Median Valley Wall of the MARK area. Tectonophysics, 190: 31-53.

Miyashiro A., Shido F. and Ewing M., 1969. Composition and origin of serpentinites from the Mid-Atlantic Ridge near 24 and 30°N. Contrib. Mineral. Petrol., 23: 117-127.

Nelson B. W. and Roy R., 1958. Synthesis of the chlorites and their structural and chemical constitution. Amer. Mineral., 43, 707 pp.

Nicolas A., and Poirier J.P., 1976. Crystalline plasticity and solid state flow in metamorphic rocks. John Wiley & Sons, London, 444 pp.

Panseri M., Fontana E. and Tartarotti P., 2008. Evolution of rodingitic dykes: metasomatism and metamorphism in the Mount Avic serpentinites, Alpine ophiolites, southern Aosta Valley. Ofioliti, 33, this volume.

Passchier C.W. and Trouw R.A.J., 1998. Micro-tectonics. Springer-Verlag, Berlin, 289 pp.

Pfeifer H.R., Colombi A. and Ganguin J., 1989. Zermatt-Saas and Antrona Zone: a petrographic and geochemical comparison of polyphase metamorphic ophiolites of the West-Central Alps. Schweiz. Mineral. Petrogr. Mitt., 69 (2): 217-236.

Piccardo G.B., Rampone E. and Scambelluri M., 1988. The Alpine evolution of the Erro-Tobbio peridotites (Voltri massif-Ligurian Alps): some field and petrographic constraints. Ofioliti, 13: 169-174.

Piccardo G.B., Zanetti A. and Müntener O., 2007. Melt/peridotite interaction in the Southern Lanzo peridotite: field, textural and geochemical evidence. Lithos, 94 (1-4): 181-209.

Piccardo G.B., Zanetti A., Spagnolo G. and Poggi E., 2005. Recent researches on melt-rock interaction in the Lanzo South peridotite. Ofioliti, 30 (2): 135-160.

Platt J.P., 1986. Dynamics of orogenic wedges and the uplift of high-pressure metamorphic rocks. Geol. Soc. Am. Bull., 97 (9): 1037-1053.

Pognante U., 1979. The Orsiera-Rocciavré ophiolitic complex (Italian Western Alps). Ofioliti, 4: 183-198.

Polino R., Gosso G. and Dal Piaz G.V., 1990. Tectonic erosion of the Adria margin and accretionary processesfor the Cretaceous orogeny of the Alps. In: F. Roure, P. Heitzmann and R. Polino (Eds.), Mem. Soc. Géol. France, N. S., 56: 345, 367.

Pouchou J.L. and Pichoir F., 1985. PAP'? (?Z) procedure for improved quantitative microanalysis. In: J.T. Armstrong (Ed.), Microbeam analysis. San Francisco Press, San Francisco, p. 104-106.

Prichard H.M., 1979. A petrographic study of the process of serpentinization in ophiolites and the ocean crust. Contrib. Mineral. Petrol., 68 (3): 231-241.

Rahn M.K. and Bucher K., 1998. Titanian clinohumite formation in the Zermatt-Saas ophiolites, Central Alps. Mineral. Petrol., 64: 1-13.

Reddy S.M., Wheeler J. and Cliff R.A., 1999. The geometry and timing of orogenic extension: an example from the Western Italian Alps. J. Metam. Geol., 17 (5): 573-589.

Reinecke T., 1998. Prograde high- to ultrahigh-pressure metamorphism and exhumation of oceanic sediments at Lago di Cignana, Zermatt-Saas zone, Western Alps. Lithos, 42: 147-189.

Ribeiro Da Costa I., Barriga F.J.A.S., Viti C., Mellini M. and Wicks F.J., 2008. Antigorite in deformed serpentinites from the Mid-Atlantic Ridge. Eur. J. Mineral., 20: 563-572.

Robinson P., 1980. The composition space of terrestrial pyroxenes-internal and external limits. In: C.T. Prewitt (Ed.), Reviews in mineralogy, 7, Pyroxenes. Min. Soc. Am., p. 419-494.

Sartori M., 1987. Structure de la zone du Combin entre les Diablons et Zermatt (Valais). Ecl. Geol. Helv., 80 (3): 789-814.

Scambelluri M., Müntener O., Ottolini L., Pettke T.T. and Vannucci R., 2004. The fate of B, Cl and Li in the subducted oceanic mantle and in the antigorite breakdown fluids. Earth Planet. Sci. Lett., 222 (1): 217-234.

Scambelluri M., Piccardo G.B., Philippot P., Robbiano A. and Negretti L., 1997. High salinity fluid inclusions formed from recycled seawater in deeply subducted alpine serpentinite. Earth Planet. Sci. Lett., 148: 485-499.

Scambelluri M. and Rampone E., 1999. Mg-metasomatism of oceanic gabbros and its control on Ti-clinohumite formation during eclogitization. Contrib. Mineral. Petrol., 135 (1): 1-17.

Scambelluri M., Rampone, E. and Piccardo, G.B., 2001. Fluid and element cycling in subducted serpentinite: a trace-element study of the Erro-Tobbio high-pressure ultramafites (Western Alps, NW Italy). J. Petrol., 42 (1): 55-67.

Siivola J. and Schmid R., 2007. List of mineral abbreviations - systematic nomenclature for metamorphic rocks: 12. Recommendations by the IUGS Subcommission on the Systematics of Metamorphic Rocks. Recommendations, web version of 01.02.2007.

Spear F.S, 1994. Metamorphic phase equilibria and pressure-temperature-time paths. Miner. Soc. Am., Washington, D.C., 799 pp.

Stampfli G., Marcoux J. and Baud A., 1991. Tethyan margins in space and time. Palaeo., Palaeo., Palaeo., 87 (1-4): 373-409.

Tartarotti P., Benciolini L. and Monopoli B., 1998. Brecce serpentinitiche nel massiccio ultrabasico del Monte Avic (Falda Ofiolitica Piemontese): possibili evidenze di erosione sottomarina. Atti Ticinensi Sci. Terra, 7: 73-86.

Tartarotti P., Susini S., Nimis P. and Ottolini L., 2002. Melt migration in the upper mantle along the Romanche fracture Zone (Equatorial Atlantic). Lithos, 63: 125-149.

Trommsdorff V. and Evans B.W., 1980. Titanian hydroxyl-clinohumite: formation and breakdown in antigorite rocks (Malenco, Italy). Contrib. Mineral. Petrol., 72: 229-242.

Ulmer P. and Trommsdorf V.,1995. Serpentine stability to mantle depths and subduction-related magmatism. Science, 268: 858-861.

Vannay J.C. and Allemann R., 1990. La zone piémontaise dans le Haut-Valtournanche (Val d'Aoste, Italie). Ecl. Geol. Helv.,83 (1): 21-39.

Wicks F.J. and O'Hanley D.S., 1988. Serpentine minerals; structures and petrology. Rev. Mineral., 19: 91-167.

Wicks F.J. and Whittaker E.J.W., 1977. Serpentine textures and serpentinization. Can. Mineral., 15: 459-488.

Wiewiora A. and Weiss Z., 1990. Crystallochemical classifications of phyllosilicates based on the unified system of projection of chemical composition: II. The chlorite group. Clay Mineral. 25: 83-92.

Wunder B. and Schreyer W., 1997. Antigorite: High-pressure stability in the system MgO-SiO_2–H_2O (MSH). Lithos, 41: 213-227.

Received, April 14, 2008
Accepted, November 25, 2008